

Figure 2. Steady-state spatial profiles of predicted for two bubble column reactor configurations (conventional, liquid recycle) with and without hydrodynamics. (a) Biomass production rate; (b) Dissolved CO concentration; (c) Gas-phase CO concentration; (d) Acetate production rate; (e) Ethanol production rate; (f) 2,3-butanediol production rate. The liquid phase exited the column at $z = 0$ m and the gas phase exited the column at $z = 10$ m. Liquid-phase concentration profiles for the recycle reactors were flat due to the assumption of homogeneity, while the conventional reactors produced spatially varying profiles.

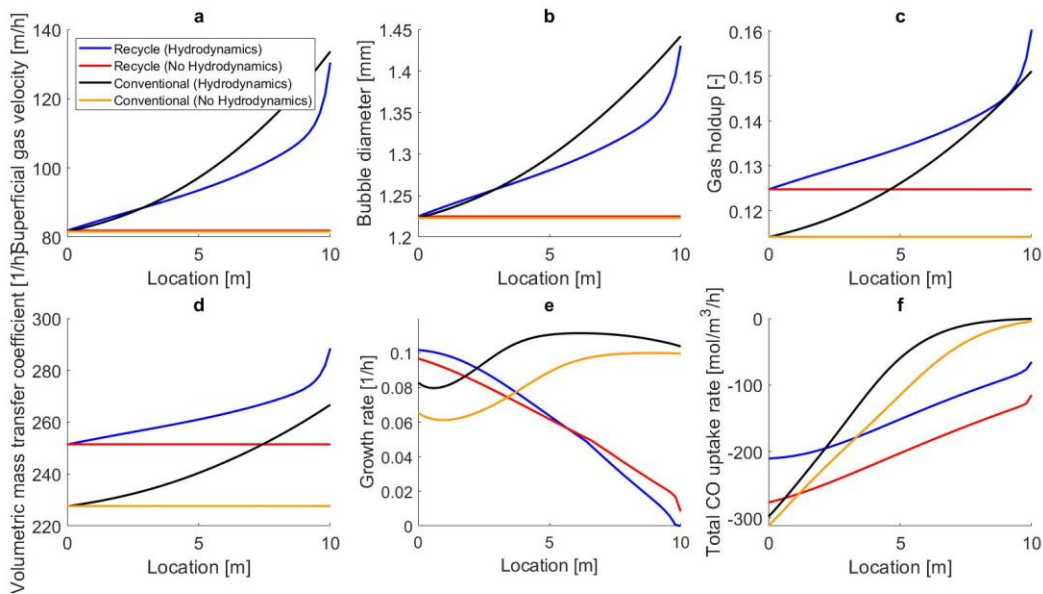


Figure 3. Steady-state spatial profiles predicted for two bubble column reactor configurations (conventional, liquid recycle) with and without hydrodynamics. (a) Superficial gas velocity; (b) Gas bubble diameter; (c) Gas holdup; (d) CO gas-liquid mass transfer; (e) *C. autoethanogenum* growth rate; (f) *C. autoethanogenum* total volumetric CO uptake rate.

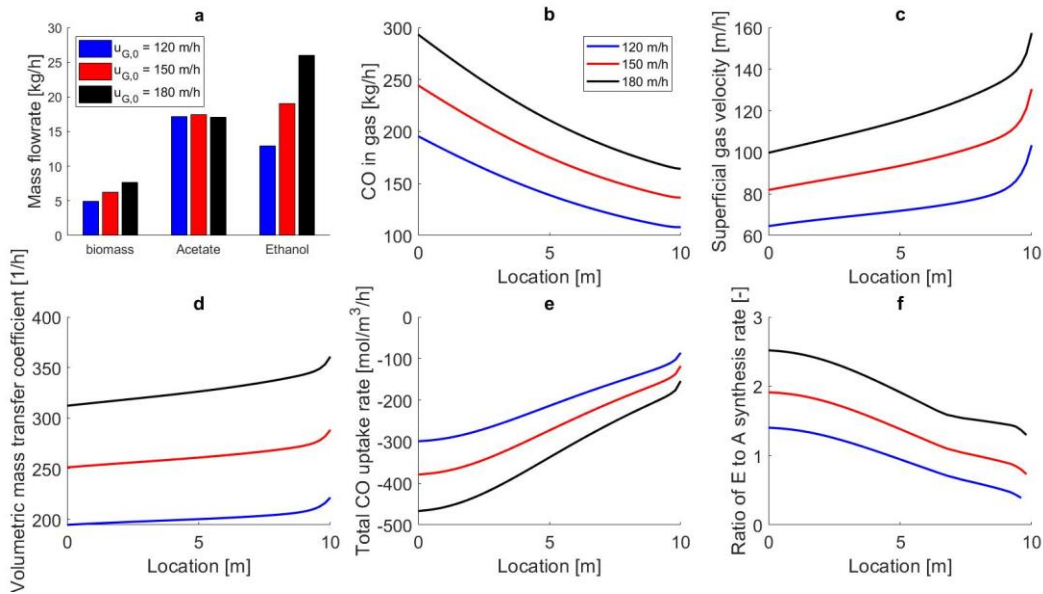


Figure 4. Effect of the feed superficial gas velocity ($u_{G,0}$) on bubble column reactor performance. The nominal value of $u_{G,0}$ was 150 m/h. (a) Biomass, acetate and ethanol mass flow rates exiting the column; (b) Gas-phase CO mass flow rate; (c) Superficial gas velocity; (d) CO gas-liquid mass transfer coefficient; (e) Total volumetric CO uptake rate; (f) Ratio of ethanol-to-acetate synthesis rate.

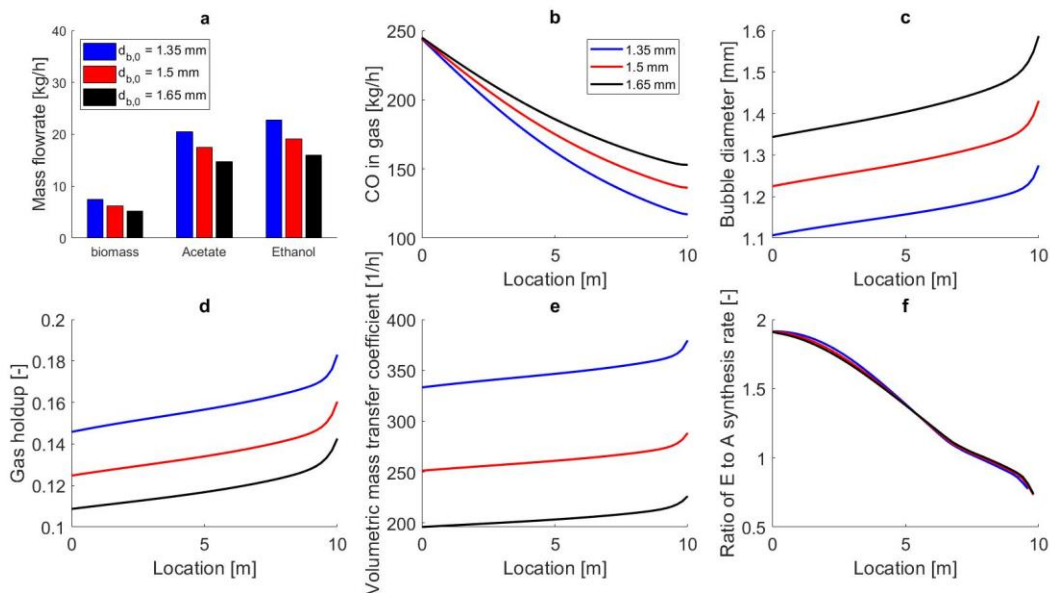


Figure 5. Effect of the feed gas bubble diameter ($d_{b,0}$) on bubble column reactor performance. The nominal value of $d_{b,0}$ was 1.5 mm. (a) Biomass, acetate and ethanol mass flow rates exiting the column; (b) Gas-phase CO mass flow rate; (c) Superficial gas velocity; (d) Gas holdup; (e) CO gas-liquid mass transfer coefficient; (f) Ratio of ethanol-to-acetate synthesis rate.

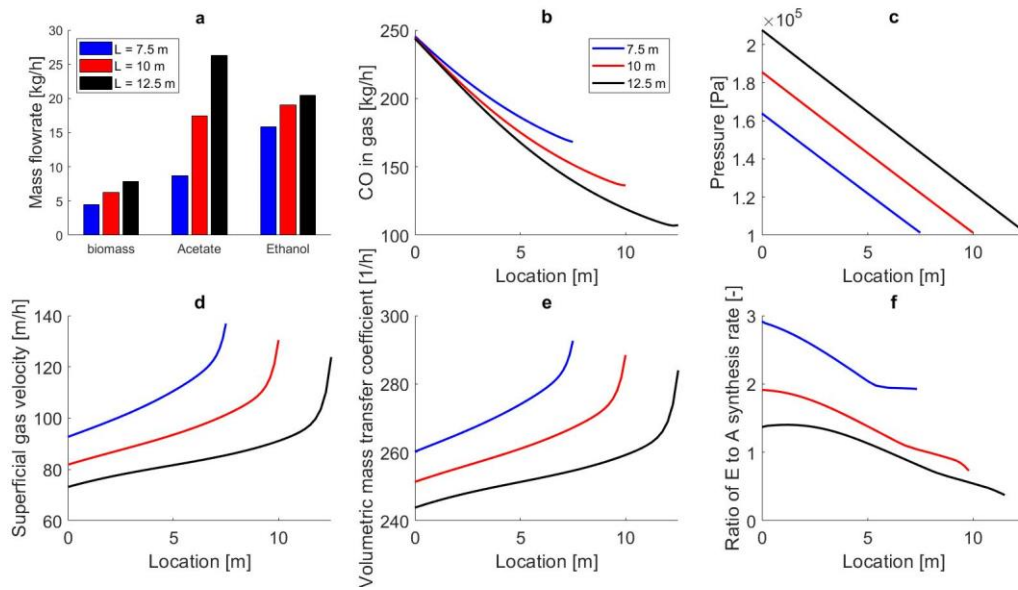


Figure 6. Effect of the column height (H) on bubble column reactor performance. The nominal value of H was 10 m. (a) Biomass, acetate and ethanol mass flow rates exiting the column; (b) Gas-phase CO mass flow rate; (c) Hydrostatic pressure; (d) Superficial gas velocity; (e) CO gas-liquid mass transfer coefficient; (f) Ratio of ethanol-to-acetate synthesis rate.

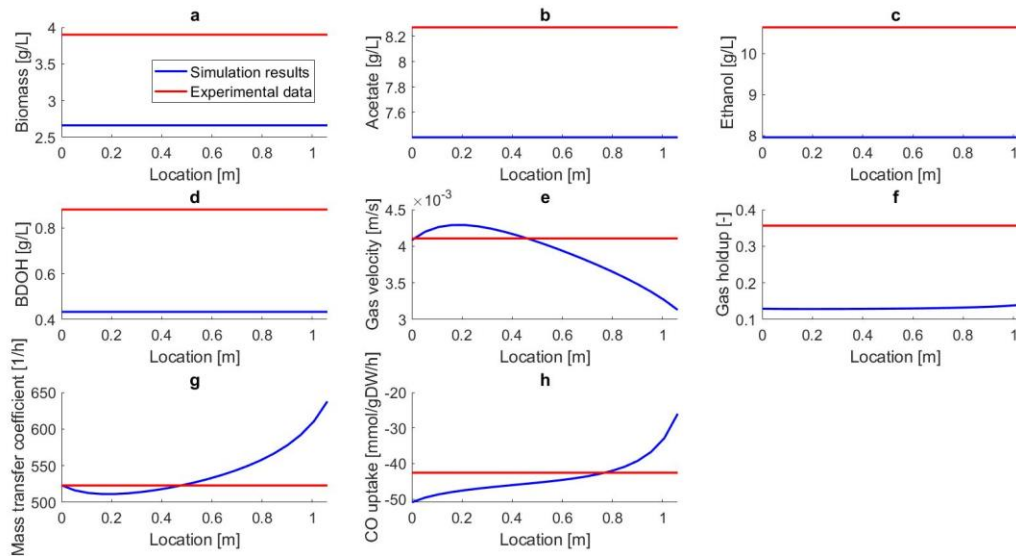


Figure S1. Comparison of model predictions obtained with an adapted version of the liquid recycle column model with hydrodynamics and experimental data of steady state 2 from our previous study (Chen et al., 2018). (a) Biomass concentration; (b) Acetate concentration; (c) Ethanol concentration; (d) 2,3-butandiol concentration; (e) Superficial gas velocity; (f) Gas holdup; (g) CO gas-liquid volumetric mass transfer coefficient; (h) CO specific uptake rate.

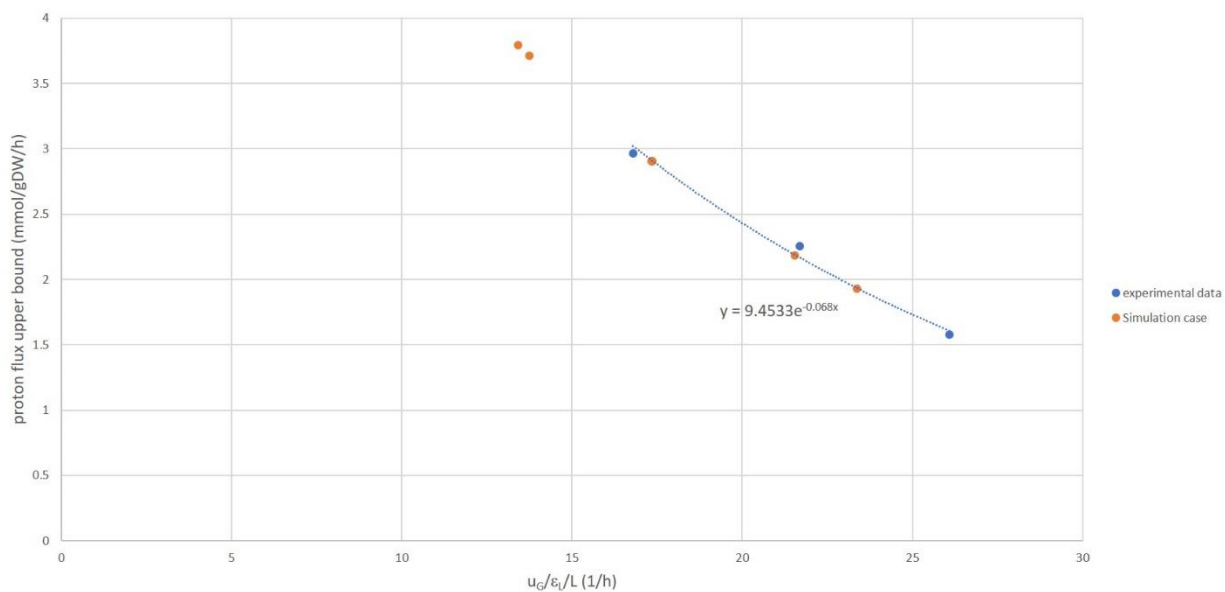


Figure S2. Exponential correlation for the upper bound of the specific proton flux used in the *C. autoethanogenum* metabolic reconstruction to improve prediction of the ethanol-acetate selectivity.

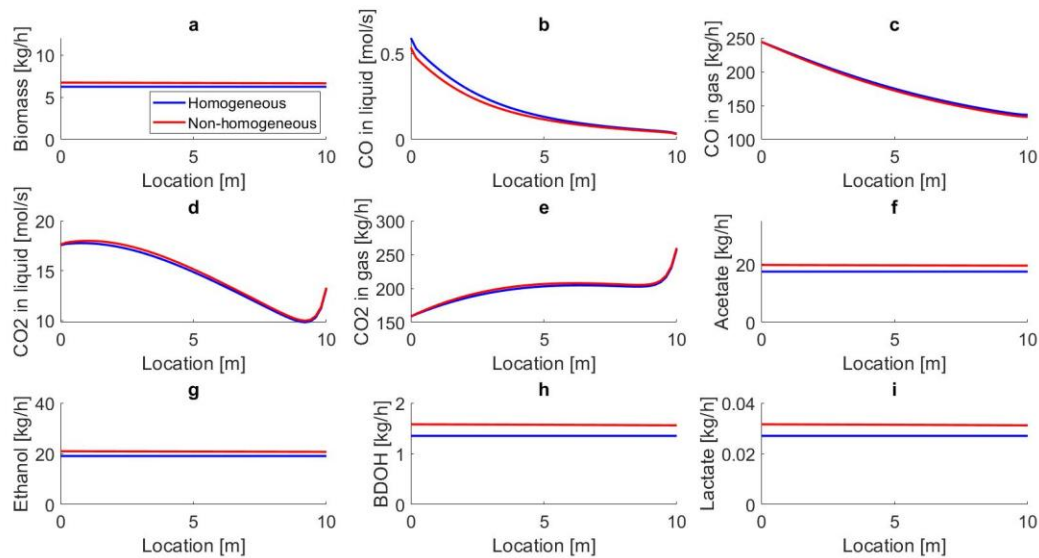


Figure S3. Comparison of steady-state predictions obtained with liquid recycle column models with hydrodynamics for homogeneous and non-homogeneous liquid phases.

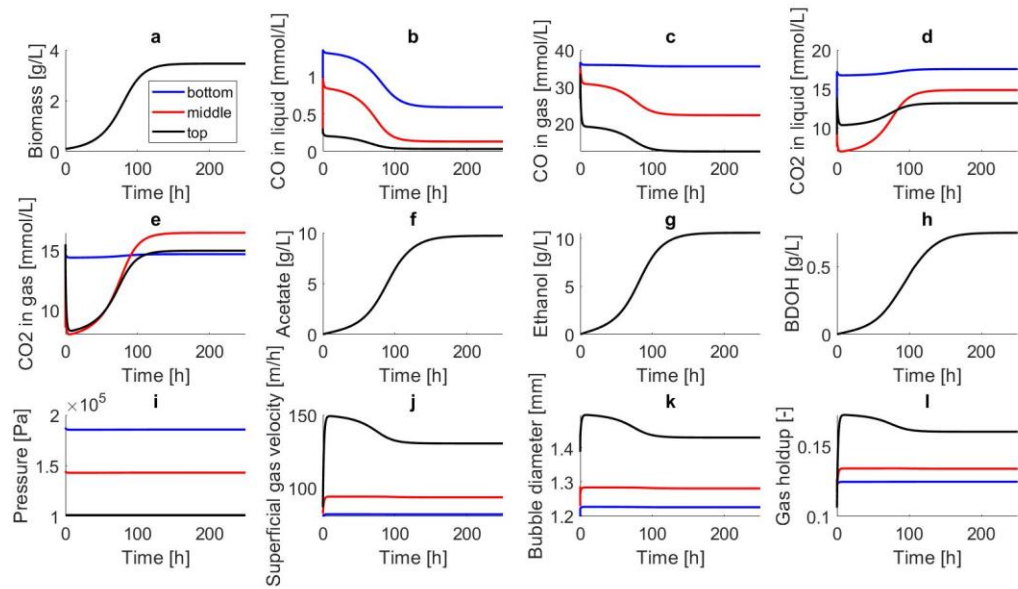


Figure S4. Comparison of steady-state predictions obtained with liquid recycle column models with hydrodynamics for homogeneous and non-homogeneous liquid phases.

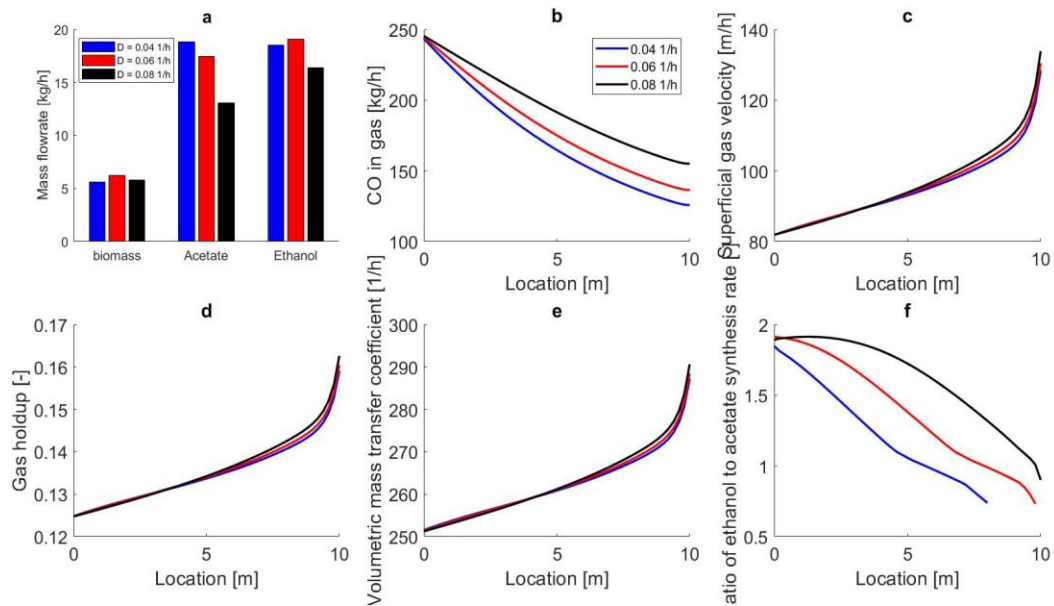


Figure S5. Steady-state predictions obtained with the liquid recycle column model with hydrodynamics for three values of the dilution rate.

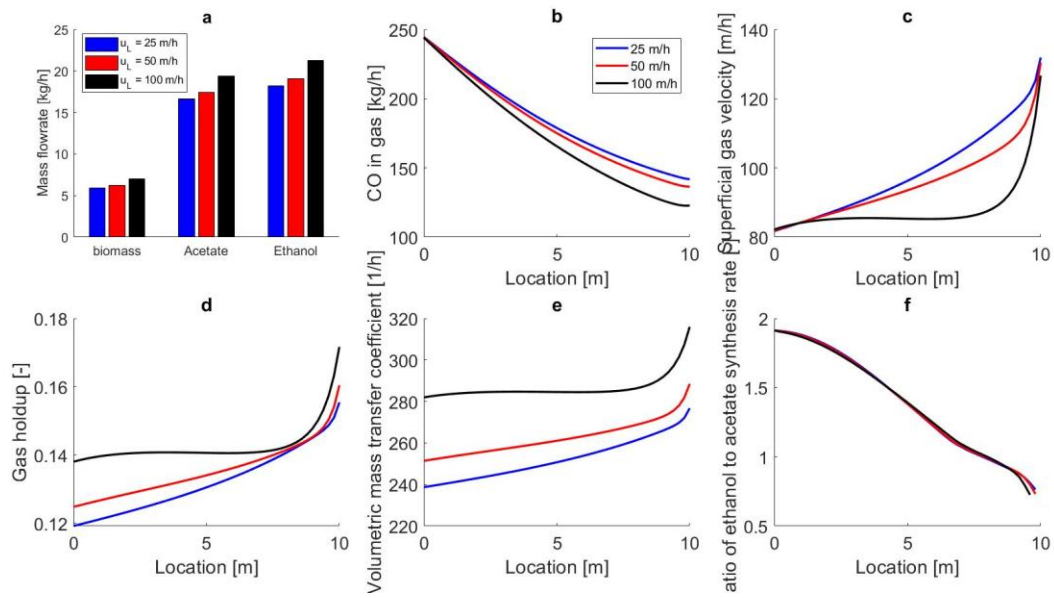


Figure S6. Steady-state predictions obtained with the liquid recycle column model with hydrodynamics for three values of the superficial liquid velocity.

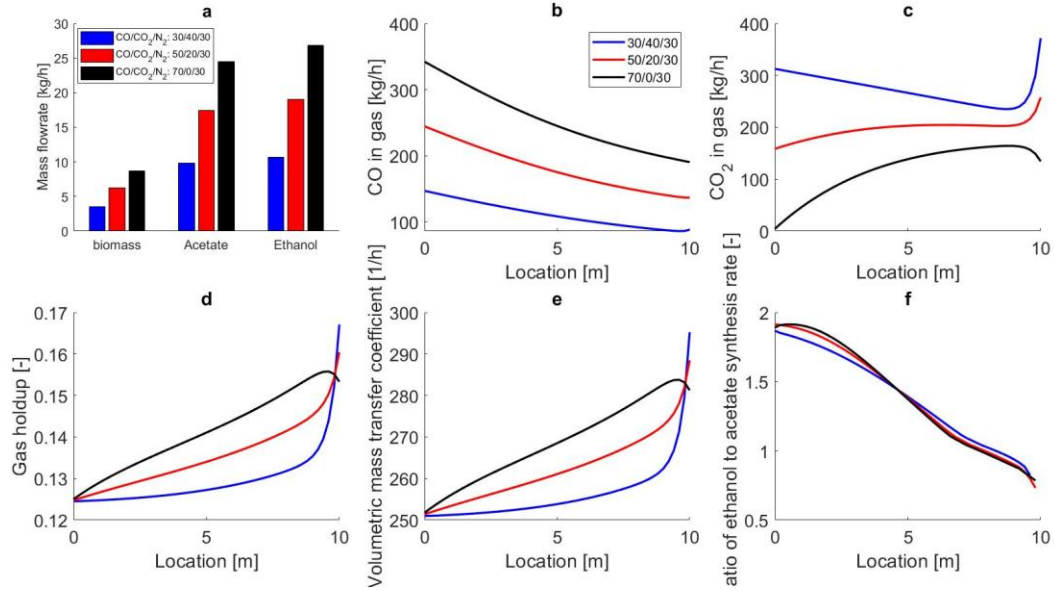


Figure S7. Steady-state predictions obtained with the liquid recycle column model with hydrodynamics for three feed gas compositions.

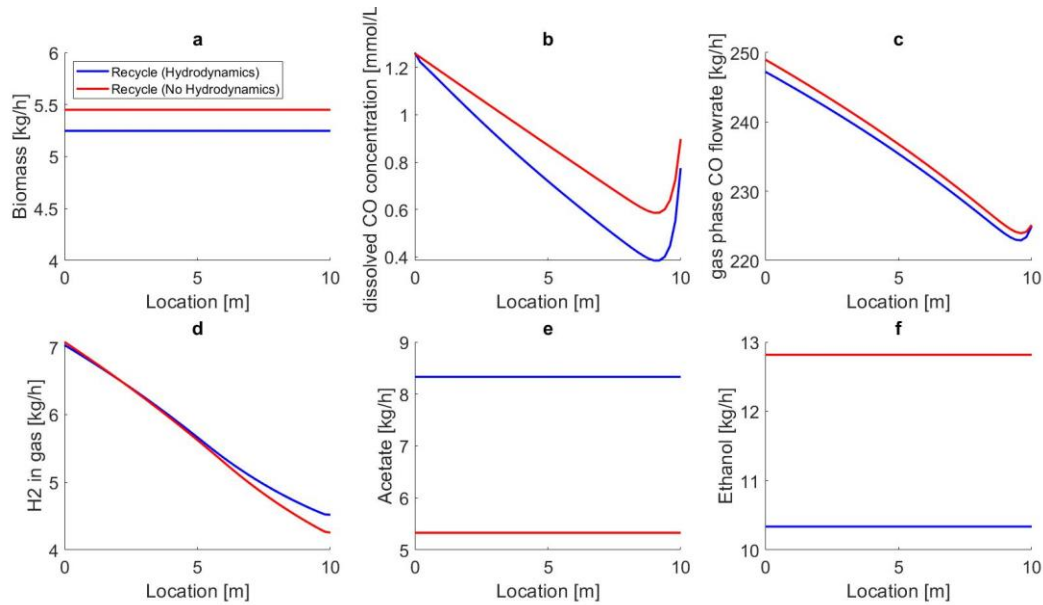


Figure S8. Steady-state spatial profiles predicted with the *C. ljungdahlii* bubble column model for the liquid recycle configuration with and without hydrodynamics. (a) Biomass production rate; (b) dissolved CO concentration; (c) gas-phase CO concentration; (d) gas-phase H₂ concentration; (e) acetate production rate; (f) ethanol production rate.

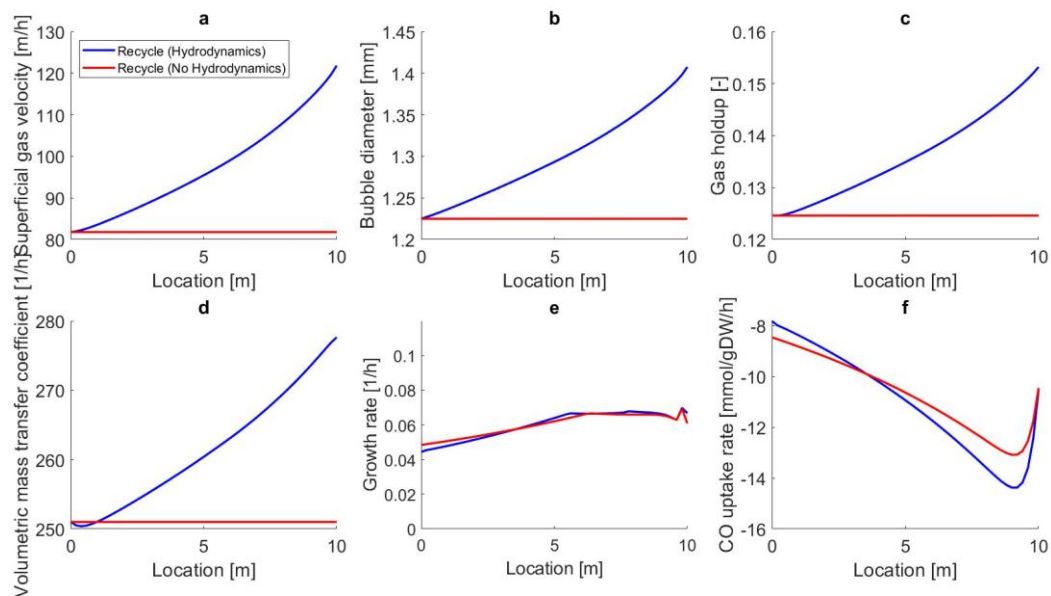


Figure S9. Steady-state spatial profiles predicted with the *C. ljungdahlii* bubble column model for the liquid recycle configuration with and without hydrodynamics. (a) Superficial gas velocity; (b) gas bubble diameter; (c) gas holdup; (d) CO gas-liquid volumetric mass transfer coefficient; (e) *C. ljungdahlii* specific growth rate; (f) *C. ljungdahlii* total CO uptake rate.